Dose saving and scatter reduction in Volume-of-Interest (VOI) cone beam CT- work in progres

Chao-Jen Lai*, Chris C. Shaw, Lingyun Chen, Xinming Liu, Tao Han, and Tianpeng Wang

Digital Imaging Research Lab, Department of Imaging Physics
The University of Texas M. D. Anderson Cancer Center, Houston, TX, USA 77030

ABSTRACT

In this study, we investigated the magnitude of scattered radiation and beam quality on the low contrast performance in cone beam breast CT imaging with applying volume-of-interest (VOI) imaging technique. For experiments, we used our bench-top cone beam CT (CBCT) system with a flat-panel digital detector. A cylindrical polycarbonate phantom of 11 cm in diameter was used to simulate breasts to measure radiation dose, scatter-to-primary-ratio (SPR), and contrast-to-noise ratio. To implement the VOI scanning technique, a lead filter with a rectangular opening was placed between the x-ray source and the breast phantom. The x-ray tube voltage setting was 80 kVp. The breast phantom was imaged without and with the VOI filter for open filed and VOI field, respectively. Dose measurement was performed using TLD dosimeters. Slot scanning technique with varying slot width was used to measure SPR values. The image quality assessment was performed based on figure of merit (FOM). The results showed that dose can be reduced by a factor of 3 or more outside the VOI and by a factor of 1.6 at the center of the phantom. The SPR value could be reduced by a factor of 9 inside the VOI, and the FOM was improved by a factor of 1.8 at the center of the phantom.

Keywords: cone beam CT, volume-of-interest, scatter-to-primary ratio, dose

1. INTRODUCTION

Mammography is the major tool for the screening and diagnosis of breast cancer. However, the detection of breast cancer on mammograms is limited by scattered radiation, noise, and overlapping anatomy. To overcome the limitation of overlapping anatomy, one of the possible solutions was proposed, cone beam breast computed tomography. Due to the advent of flat panel (FP) image detector, the combination of FP detector and CBCT provides a true 3D volumetric image. Cone beam breast CT techniques with dedicated pendant geometry have been proposed and investigated by several researchers [1-4]. As a part of effort, a bench-top CBCT system has been built in our lab and used to scan mastectomy breasts.

Although cone beam breast CT can provide high tissue contrast and true 3-D images of the breast anatomy, scattered radiation is still a major problem for CBCT breast imaging due to the use of an area detector for image acquisition. This scatter component can introduce additional noise to the image signals in the projection images, resulting in underestimation of the CT numbers and degraded image quality. In addition, depending on the tasks (such as screening, diagnosis, treatment planning), the limit of radiation dose is required. Therefore, keeping radiation dose as low as possible to the surrounding cancer areas is preferable. Volume-of-interest (VOI) imaging technique was thus proposed to image phantom with substantial reduced dose outside the VOI and to obtain an acceptable image quality inside the VOI in the reconstructed image [5,6]. In this paper, dose and scatter-to-primary ratio (SPR) measurements were performed without and with employing VOI imaging technique.

* chaolai@di.mdacc.tmc.edu; phone (713) 745-2837; fax (713) 563-9328

Medical Imaging 2008: Physics of Medical Imaging, edited by Jiang Hsieh, Ehsan Samei,
Proc. of SPIE Vol. 6913, 69134V, (2008) · 1605-7422/08/$18 · doi: 10.1117/12.772807

2. MATERIALS AND METHODS

2.1 Imaging system

An experimental cone beam breast CT system was constructed on an optical bench in our lab (fig. 1). The system consisted of a three phase high frequency generator (INDICO 100, CPI Canada Inc., Ontario, Canada) coupled with a dual focal spot x-ray tube (G1592, Varian Medical Systems, Salt Lake City, UT), an a-Si:H/CsI(Tl) based FP detector (Paxscan 4030CB, Varian Medical Systems), and a motorized rotating table. The focal spot size used in this study is 0.6 mm. The active matrix of the FP detector is 2048×1536 pixels with a pixel pitch of 194 μm. For imaging studies, a uniform cylindrical polycarbonate (lexan) phantom of 11 cm in diameter was used to simulate soft tissue. The phantom consisted of 2 identical size cylinders, one in 2.54 cm thick with 3 through-hole at its symmetry axis to place Thermoluminescent dosimeter (TLD) and to inject low-contrast liquid and the other in 10 cm thick with a whole piece. They were stacked together and put on the rotating table for the imaging experiments.

The focal spot plane was aligned at the middle plane of the FP detector (fig. 1). The x-ray source-to-isocenter distance (SCD) was 75 cm, and the distance between the x-ray source and the FP detector (SID) was 100 cm. Therefore, the magnification, defined as the ratio of the SID to the SCD, is 1.33 in this study. The x-ray tube voltage setting was 80 kVp. For mimicking pendant geometry, 3 mm thick lead was used to block half of x-ray beam (fig. 1) to form a half-cone beam for scanning breasts. For VOI technique, a 2.25 mm thick with a rectangular opening was used as the VOI filter. The VOI filter was placed between x-ray tube and the phantom. Moving position for the VOI filter to obtain the VOI opening size was 2.5 cm at the isocenter plane.

2.2 Dose and CNR measurements

TLDs were placed at 3 locations in the phantom (fig. 2) and positioned near the focal spot plane. The x-ray generator was operated in pulsed mode at 7.5 pulses per second and supplied the clock signals to sync the flat panel detector frame acquisition and triggered the rotary stage motion. The x-ray pulse width and current were set to 30 msec and 25 mA, respectively. The phantom was exposed 2 minutes, which was equal to 3 scanning rotations, without VOI filter present. Similarly, the phantom was imaged repeatedly while the VOI filter was employed. These TLDs were read using TLD reader (Harshaw 3500 TLD reader, Harshaw-Bicron, Newbury, OH).

In order to evaluate low contrast performance, water was injected into these locations. 300 projection views were then acquired for each condition. The CT reconstruction for open field was performed using the FDK filtered backprojection algorithm [7]. The VOI reconstructed CT image was obtained by two steps: (1) projection views were preprocessed with low exposure images and (2) applying FDK filtered backprojection algorithm for the preprocessed projection views. The pixel size and the slice thickness of the reconstructed images were set to 145 μm. The contrast-to-noise ratio (CNR) values were calculated for water located at in the center of the phantom without and with the VOI filter present. To compare CNR values as a function of beam quality, figure of merit (FOM) metric was calculated using the following formula:

$$FOM = \frac{I_w - I_P}{\sigma_P \sqrt{D}} \qquad (1)$$

Where I_P and σ_P were the mean and standard deviation of the linear attenuation coefficient of the phantom, I_W is the mean linear attenuation coefficient of water, and D is absorbed dose.

2.3 SPR measurement

To investigate the magnitude of scatter, SPR measurement was performed at the detector plane by using a slot scanning device positioned close to the x-ray tube. For each measurement of SPR (slot width), twenty projection images were acquired three time. Image signal within the slot consists of primary and scatter signals. In addition, the amount of scatter introduced to the image signal was varied by adjusting slot width. The image signals as function of slot width.

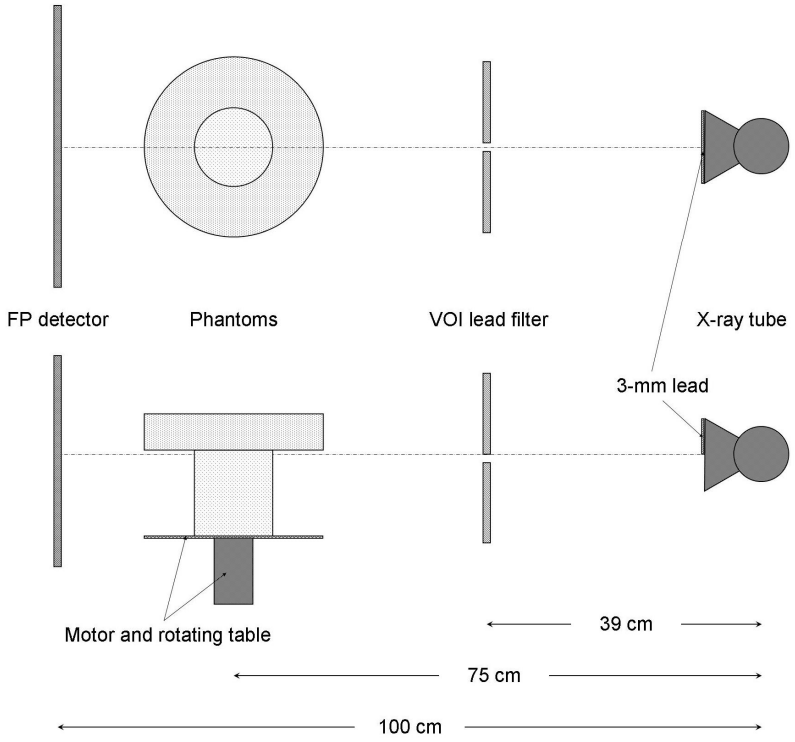

Fig. 1 Experimental setup of CBCT system in our lab for dose and CNR measurements. A slot scanning device was placed between the x-ray tube and VOI filter for SPR measurement.

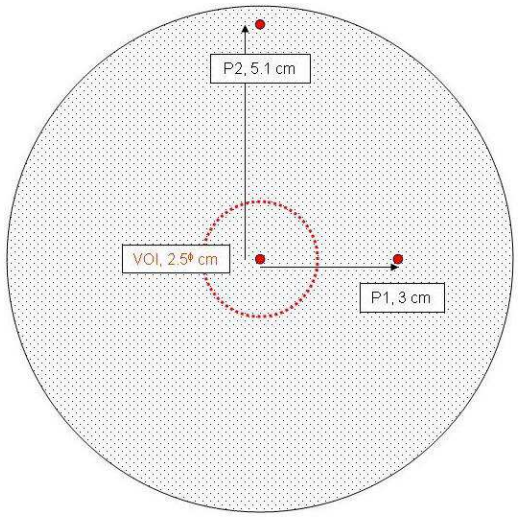

Fig. 2 The cross section of the phantom used to perform dose and CNR measurements near focal spot plane.

		Open field	VOI field
Dose (mGy)	Center	14	8.7
	P1	15.7	4.3
	P2	19.6	3.5
FOM	Center	0.235 (0.023)	0.433 (0.020)

Table 1 Doses measured at 3 locations of the phantom for the open field and the VOI field. The numbers in the parenthesis are the standard deviation.

		Open field	VOI field
SPR	Center	0.375 (0.007)	0.028 (0.005)
	P1	0.254 (0.004)	0
	P2	0.098 (0.005)	0

Table 2 SPR values measured at 3 locations of the phantom for the open field and the VOI field. The numbers in the parenthesis are the standard deviation.

were used to estimate primary signal, and the scatter signal was obtained by subtracting from the image signal for each slot width. The estimated SPR was then obtained by dividing the scatter signal by the primary signal for each slot width. After that, these estimated SPR values were plotted as function of image signals and were used to compute the primary signal using extrapolation method while the SPR equal to zero. The SPR for open field was calculated by dividing the difference between the image signal (from open field) and primary signal by the primary signal. Similar measurement was performed while the VOI filter was present.

3. RESULTS and DISCUSSION

3.1 Dose and FOM measurements

Table 1 lists the dose measurement for the both fields. It was found that the dose increased as away from the center for the open filed but decreased for the VOI filed. This is because P1 and P2 were outside the VOI. It was found that the dose is reduced by a factor of ~3.7 and ~5.5 for P1 and P2 locations, respectively. In addition, the VOI field has lower dose than the open field at the center location. The dose reduction factor is about 1.6. This may be due to less scatter at the center location. This was confirmed with the image signal profiles. Inside the VOI, the image signals were around 610 and 440 for the open field and the VOI field, respectively. This indicates that the image signal increases ~38% due to scatter radiation. These two reduction factors are different, which can be explained due to self-shielding by the phantom.

The FOM, defined in Eq. (1), was computed from two reconstructed CT images, and the average FOM values were 0.235 (±0.023) and 0.433 (±0.020) for the open field and the VOI field, respectively. This result shows that the FOM inside the VOI improves ~80%. This may be due to scatter reduction with the VOI filter even though noise was introduced into the VOI image. The result also implies that lower dose can be applied to the VOI technique to obtain equal FOM values compared to the open field. However, further investigation is needed.

3.2 SPR measurement

Table 2 lists the SPR values at the three locations (same as dose measurement) for the open field and at the center of the phantom for the VOI field. It was found that the SPR has the highest measure around the center of the phantom (~0.4) and decreases toward the edge gradually. In addition, the ranges of the SPR inside the VOI were 0.35-0.39 and 0.025-0.053 for the open filed and the VOI field, respectively. This indicates that the SPR can be reduced by a factor of ~9.5 due to smaller field of view.

4. CONCLUSIONS

We studied the magnitude of scattered radiation and beam quality on the low contrast performance associated with the dose measurement for VOI imaging technique. It is significant that, compared to the open field, dose can be reduced by a factor of 3 or more outside the VOI, dependent on the location, and by a factor of 1.6 at the center of the phantom. In addition, the SPR value can be reduced by a factor of 9 inside the VOI. Furthermore, the image quality index, FOM, can be improved by a factor of 1.8 at the center of the phantom. These results show that the VOI imaging technique is a promising method to improve image quality with significant scatter rejection and dose reduction.

ACKNOWLEDGMENTS

This work was supported in part by a research grant EB-00117 from the National Institute of Biomedical Imaging and Bioengineering and a research grant ca104759 from the National Cancer Institute.

REFERENCES

1. B. Chen and R. Ning, "Cone-beam volume CT breast imaging: feasibility study," *Med. Phys.* **29**, p. 755-770, 2002.
2. X. Gong, A.A. Vedula, and S.J. Glick, "Microcalcification detection using cone-beam CT mammography with a flat-panel imager," *Phys. Med. Biol.* **49**, p. 2183-2195, 2004.
3. J.M. Boone, N. Shah, and T.R. Nelson, "A comprehensive analysis of DgN(CT) coefficients for pendant-geometry cone-beam breast computed tomography," *Med. Phys.* **31**, p. 226-235, 2004.
4. C.-J. Lai, C.C. Shaw, L. Chen, M.C. Altunbas, X. Liu, T. Han, T. Wang, W.T. Yang, G.J. Whitman, and S.-J. Tu, "Visibility of microcalcification in cone beam breast CT: effects of X-ray tube voltage and radiation dose," *Med. Phys.* **34**, p. 2995-3004, 2007.
5. R. Chityala, K.R. Hoffmann, D.R. Bednarek, and S. Rudin, "Region of interest (ROI) computed tomography," *Proc. SPIE* **5368**, p. 534-541, 2004.
6. L. Chen, C.C. Shaw, M.C. Altunbas, T. Wang, S.-J. Tu, C.-J. Lai, X. Liu, "A volume-of-interest (VOI) scanning technique for cone beam breast CT," *Med. Phys.* **32**, p. 2064, 2005.
7. L.A. Feldkamp, L.C. Davis, and J.W. Kress, "Practical cone-beam algorithm," *J. Opt. Soc. Am. A* **1**, p. 612-619, 1984.